Robust LQR Control for PWM Converters:
An LMI Approach

Carlos Olalla, *Student Member, IEEE*, Ramon Leyva, *Member, IEEE*,
Abdelali El Aroudi, *Member, IEEE*, and Isabelle Queinnec

Abstract—**A consistent framework for robust linear quadratic regulators (LQRs) control of power converters is presented. Systems with conventional LQR controllers present good stability properties and are optimal with respect to a certain performance index. However, LQR control does not assure robust stability when the system is highly uncertain. In this paper, a convex model of converter dynamics is obtained taking into account uncertainty of parameters. In addition, the LQR control for switching converters is reviewed. In order to apply the LQR control in the uncertain converter case, we propose to optimize the performance index by using linear matrix inequalities (LMIs). As a consequence, a new robust control method for dc–dc converters is derived. This LMI-LQR control is compared with classical LQR control when designing a boost regulator. Performance of both cases is discussed for load and line perturbations, working at nominal and nonnominal conditions. Finally, the correctness of the proposed approach is verified with experimental prototypes.**

Index Terms—**Optimal control, power electronics, robustness.**

I. INTRODUCTION

SWITCHED-MODE dc–dc converters are used extensively in modern power electronics devices due to their high efficiency, low cost, and small size [1]. In order to protect the source and the load, the dynamic behavior of the switched-mode converters is driven by means of a control subsystem. The control law obtained for these control subsystems is usually based on linear output or state feedback, which is simpler and of lower cost than other nonlinear approaches, despite that the converter dynamics are nonlinear due to switching action, feedback, and saturation of the duty-cycle. The control objectives of such devices are 1) to maintain a stable regulation of the output voltage, 2) to maximize the bandwidth of the closed-loop system in order to reject disturbances, as well as 3) to satisfy desirable transient characteristics (as for example, to minimize output overshoot). The models used to derive the control strategy usually neglect the high-frequency ripple considering that the switching time is small enough. Usually, such averaged

models are linearized at a certain operation point in order to derive a linear controller. Nevertheless, a design that disregards converter nonlinearities may result in deteriorated output signal or unstable behavior in presence of large perturbations.

In order to take into account nonlinearities and parameter uncertainty, the study of converter models and robust control methods is still an active area of investigation [2]–[6]. In this paper, we will present a linear control design method based on linear quadratic regulators (LQRs), in which we achieve robust stability and performance despite model inaccuracies.

The classic LQR approach (see [7] and [8]) deals with the optimization of a cost function or performance index. Thus, the designer can weight which states and which inputs are more important in the control action to seek for appropriate transient and steady-state performances. Specifically, in the field of power conversion, the choice of the cost function parameters is advantageous, since it can be used to minimize the ripple present in the feedback signal. It is also worth to point out that the closed-loop system with such LQR controller presents interesting properties like a phase margin larger than $60°$ and an infinite gain margin. Such phase margin specification appears as a standard requirement in many power electronics applications [9]. However, unlike other current systematic control design procedures, like H_∞ or μ-synthesis, classic LQR control cannot cope with system uncertainty.

The aforementioned features of LQR control have prompted several authors to apply successfully this technique in the field of switched power converters [10]–[14]. In [10] and [11], the performance indexes are selected using pole placement relationships. In [12], the cost function is derived from an initial controller, which was obtained by frequency domain methods. Other works [13], [14] make use of simulations to find the appropriate performance indexes or arbitrarily choose them, in order to, for example, enforce integral action. In all these works, the converter model is obtained from a linearization of the averaged circuit, and consequently, the LQR control properties are not assured out of the nominal conditions. In these works, the LQR controller has been derived by solving an algebraic Riccati equation.

Nevertheless, the LQR problem can also be formulated in form of linear matrix inequalities (LMIs), and numerically solved by convex optimization methods [15]. This numerical approach has several advantages. While the algebraic solution can only be applied to one plant case, the numerical procedure can take into account multiple plants, i.e., it can cope with uncertain systems at different operation points. This approach

results in robust stability of nonlinear switched-mode converters. Aside from the robust stability, the LMI solution of the LQR problem can include other design requirements, as pole placement restrictions [16], saturation constraints [17], or energy-based specifications [18]. This approach allows the practicing engineer to combine the properties of LQR control with uncertainty and other requirements. The resulting controller is not optimal as in the nominal case, but provides an upper bound (or guaranteed cost) of the performance index. There exist other gradient-based approaches to obtain robust LQR controllers [19]. However, these approaches are not easily adaptable to additional design requirements, and they require the designer to find expressions of the differential sensitivity of the system. Finally, we propose to solve this optimization problem with an interior point algorithm [20], [21] since it is considered a very efficient numerical method in this kind of problem [15, Ch. 1].

Thus, in order to control dc–dc converters in large with robust specifications, we will formulate the LQR control of a switched-mode converter in terms of LMIs and solve it by convex optimization methods. Our contribution is to provide a compact control design procedure which is suitable for nonlinear switching sources. Other authors have also used LMI control approaches in the field of power electronics [22]. Nevertheless, our approach differs from [22] since we propose an optimal LQR controller for a boost and a buck converter while the previous work deals with a minimization of the $\mathcal{H}_\infty$ norm for the buck case. In addition, we show an experimental verification of the proposed design which is in perfect agreement with the analytical derivations.

The remaining sections are organized as follows. First, in Section II, we introduce the uncertain models of a buck and a boost converter. In Section III, we give a basic LMI control theory background, with the formulation needed to solve the LQR problem. In Section IV, we present two design examples to illustrate the advantages of this approach. In the first example, we obtain an LQR controller of an uncertain buck converter, while in the second, we build an LQR controller for an uncertain boost converter. Both examples have been simulated with a switched-mode circuit using PSIM [23]. The implementation of the second example has been deployed in Section IV, where we demonstrate the validity of this design procedure. The control scheme can be easily implemented by operational amplifiers (OAs), a pulsewidth modulation (PWM) circuit and standard analog elements. Section V summarizes the key aspects of this paper and presents some conclusions.

II. POLYTOPIC MODELING OF UNCERTAIN POWER CONVERTERS

Linearized models of switched-mode converters are sensitive to system uncertainty. The steady-state duty-cycle, the load, or the parametric uncertainty of the storage elements may change the model response considerably. For these reasons, it is of major importance that the control design procedures for power converters may permit a proper treatment of the uncertainty. In this section, we will introduce the polytopic representation of uncertainty in a buck and a boost converter.
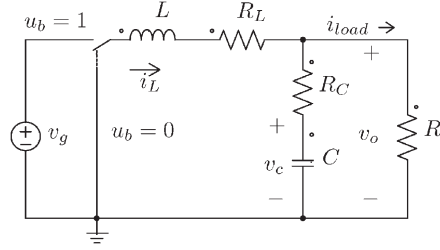

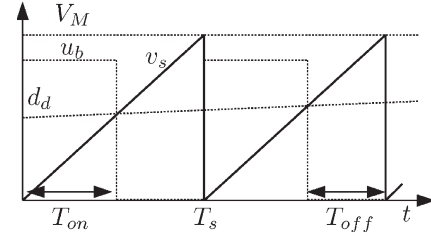Fig. 1. Schematic of the buck converter.

Fig. 2. Waveforms of the PWM process.

A. Polytopic Model of an Uncertain PWM Buck Converter

Fig. 1 shows the schematic of a dc–dc step-down (buck) converter where v_o is the output voltage and v_g is the line voltage. The output voltage must be kept at a given constant value V_{ref}. R models the converter load, while C and L represent, respectively, capacitance of the capacitor and inductance of the inductor, whose equivalent series resistances, R_C and R_L, are considered sufficiently small to be neglected. The measurable states are the inductor current i_L and the capacitor voltage v_C.

The binary signal (u_{b}) that turns on and off the switches is controlled by means of a fixed-frequency PWM (see Fig. 2). The constant switching frequency is $1/T_{\text{s}}$, where T_{s} is the switching period equal to the sum of T_{on} (when $u_{\text{b}} = 1$) and T_{off} (when $u_{\text{b}} = 0$) where the ratio $T_{\text{on}}/(T_{\text{on}} + T_{\text{off}})$ is the duty-cycle d_{d}. The duty-cycle is compared with a sawtooth signal v_{s} of amplitude $V_M = 1$. We assume that the converter operates in continuous conduction mode (CCM) and that the inductor current is not saturated.

The following expression shows the state-space averaged model of a PWM converter [24]:

$$\dot{\tilde{x}}(t) = (A_{\text{off}} - (A_{\text{on}} - A_{\text{off}})U)\,\tilde{x}(t) + (A_{\text{on}} - A_{\text{off}})\tilde{x}(t)$$
$$\times \tilde{u}(t) + ((A_{\text{on}} - A_{\text{off}})X + (B_{u_{\text{on}}} - B_{u_{\text{off}}}))\,\tilde{u}(t) \quad (1)$$

where A_{on} and $B_{u_{\text{on}}}$ are the state-space matrices during T_{on} and A_{off} and $B_{u_{\text{off}}}$ are the state-space matrices during T_{off}. The incremental and equilibrium input vectors are $\tilde{u}(t)$ and U while the incremental and equilibrium state vectors are $\tilde{x}(t)$ and X. The values of vectors and state-space matrices are written as follows:

$$\tilde{u}(t) = \tilde{d}_{\text{d}}(t) \qquad U = D_{\text{d}}$$
$$\tilde{x}(t) = \begin{bmatrix} \tilde{i}_L(t) \\ \tilde{v}_C(t) \end{bmatrix} \qquad X = \begin{bmatrix} \frac{V_{\text{g}}D_{\text{d}}}{R} \\ V_{\text{g}}D_{\text{d}} \end{bmatrix}$$
$$A_{\text{off}} = A_{\text{on}} = \begin{bmatrix} 0 & -\frac{1}{L} \\ \frac{1}{C} & -\frac{1}{RC} \end{bmatrix}$$
$$B_{u_{\text{on}}} = \begin{bmatrix} \frac{V_{\text{g}}}{L} \\ 0 \end{bmatrix} \qquad B_{u_{\text{off}}} = \begin{bmatrix} 0 \\ 0 \end{bmatrix}. \quad (2)$$

Since $A_{\mathrm{on}} = A_{\mathrm{off}}$, the averaged model of the buck converter is linear

$$\dot{\tilde{x}}(t) = \begin{bmatrix} 0 & -\frac{1}{L} \\ \frac{1}{C} & -\frac{1}{RC} \end{bmatrix} \tilde{x}(t) + \begin{bmatrix} \frac{V_g}{L} \\ 0 \end{bmatrix} \tilde{u}(t). \qquad (3)$$

This model is then augmented with an additional state variable $\tilde{x}_3(t)$ which stands for the integral of the output voltage error, i.e., $\tilde{x}_3(t) = -\int \tilde{v}_c(t)$, such that the steady-state error is zero. The augmented model is written as

$$\dot{\tilde{x}}(t) = A\tilde{x}(t) + B_u\tilde{u}(t) \qquad (4)$$

where

$$A = \begin{bmatrix} 0 & -\frac{1}{L} & 0 \\ \frac{1}{C} & -\frac{1}{RC} & 0 \\ 0 & -1 & 0 \end{bmatrix} \qquad B_u = \begin{bmatrix} \frac{V_g}{L} \\ 0 \\ 0 \end{bmatrix}. \qquad (5)$$

Some elements involved in the system matrices may be uncertain or time varying. Then, matrices A and B_u depend on such uncertain or time-varying terms, and we can express (4) as a function of these parameters

$$\dot{x}(t) = A(p)x(t) + B_u(p)u(t). \qquad (6)$$

The uncertain terms are grouped in a vector p. In a general case, the vector p consists of n_p uncertain parameters $p = (p_1, \ldots, p_{n_p})$, where each uncertain parameter p_i is bounded between a minimum and a maximum value $\underline{p_i}$ and $\overline{p_i}$

$$p_i \in [\underline{p_i} \quad \overline{p_i}]. \qquad (7)$$

In general, the admissible values of vector p are constrained in an hyperrectangle in the parameter space $\mathbb{R}^{n_p}$ with $N = 2^{n_p}$ vertices $\{v_1, \ldots, v_N\}$. The images of the matrix $[A(p), B_u(p)]$ for each vertex v_i corresponds to a set $\{\mathcal{G}_1, \ldots, \mathcal{G}_N\}$. The components of the set $\{\mathcal{G}_1, \ldots, \mathcal{G}_N\}$ are the extrema of a convex polytope which contains the images for all admissible values of p if the matrix $[A(p), B_u(p)]$ depends linearly on p

$$[A(p), B_u(p)] \in \mathrm{Co}\,\{\mathcal{G}_1, \ldots, \mathcal{G}_N\}$$

$$:= \left\{ \sum_{i=1}^{N} \lambda_i \mathcal{G}_i, \quad \lambda_i \geq 0, \quad \sum_{i=1}^{N} \lambda_i = 1 \right\}. \qquad (8)$$

For an in-deep explanation of polytopic models of uncertainty see [15, Ch. 4], [20, Ch. 2], and [25].

In this context, we consider that the load R and the line voltage V_g are uncertain parameters. We also consider that all other parameters are well known. Then, $n_p = 2$ and the parameter vector $p = [1/R \quad V_g]$, where

$$1/R \in [1/R_{\max}, 1/R_{\min}] \quad V_g \in [V_{g\min}, V_{g\max}]. \qquad (9)$$

Since the buck converter matrices A and B_u depend linearly on the uncertain parameters $1/R$ and V_g, we can define a polytope
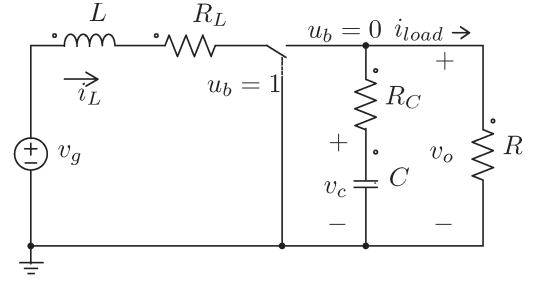

Fig. 3. Schematic of the boost converter.

of $N = 2^2$ vertices that contains all the possible values of the uncertain matrices. The vertices of the polytopic model are

$$A_1 = \begin{bmatrix} 0 & -\frac{1}{L} & 0 \\ \frac{1}{C} & -\frac{1}{R_{\max}C} & 0 \\ 0 & -1 & 0 \end{bmatrix} \quad B_{u1} = \begin{bmatrix} \frac{V_{g\min}}{L} \\ 0 \\ 0 \end{bmatrix}$$

$$A_2 = \begin{bmatrix} 0 & -\frac{1}{L} & 0 \\ \frac{1}{C} & -\frac{1}{R_{\min}C} & 0 \\ 0 & -1 & 0 \end{bmatrix} \quad B_{u2} = \begin{bmatrix} \frac{V_{g\max}}{L} \\ 0 \\ 0 \end{bmatrix}$$

$$A_3 = A_2 \qquad\qquad B_{u3} = B_{u1}$$

$$A_4 = A_1 \qquad\qquad B_{u4} = B_{u2}. \qquad (10)$$

This model will be used in Section IV to find an LQR controller for the buck converter. It is worth to point out that the same procedure can be used to take into account more uncertain terms. Nevertheless, as much uncertainty there is in the converter, lower performance level can be assured [26]. The conservatism is even increased when uncertain parameters do not appear linearly. Such case is shown in the next section, which deals with a PWM boost converter.

B. Polytopic Model of an Uncertain PWM Boost Converter

Fig. 3 shows the circuit diagram of a dc–dc step-up (boost) converter. In order to simplify the notation, we retake the naming convention of the previous example. All the assumptions made for the previous section also hold, i.e., the converter operates in CCM and the stray resistances R_C and R_L are sufficiently small to be neglected.

The averaged model of the boost converter has the form presented in (1). The state-space matrices for the boost converter are written as follows:

$$\tilde{u}(t) = \tilde{d}_{\mathrm{d}}(t) \qquad\qquad U = D_{\mathrm{d}}$$

$$\tilde{x}(t) = \begin{bmatrix} \tilde{i}_L(t) \\ \tilde{v}_C(t) \end{bmatrix} \qquad\qquad X = \begin{bmatrix} \frac{V_g}{D_{\mathrm{d}}'^2 R} \\ \frac{V_g}{D_{\mathrm{d}}'} \end{bmatrix}$$

$$A_{\mathrm{off}} = \begin{bmatrix} 0 & 0 \\ 0 & -\frac{1}{RC} \end{bmatrix} \qquad A_{\mathrm{on}} = \begin{bmatrix} 0 & -\frac{1}{L} \\ \frac{1}{C} & -\frac{1}{RC} \end{bmatrix}$$

$$B_{u_{\mathrm{on}}} = B_{u_{\mathrm{off}}} = \begin{bmatrix} \frac{1}{L} \\ 0 \end{bmatrix} \qquad\qquad (11)$$

where D_{d}' is the complementary operating point duty-cycle $D_{\mathrm{d}}' = 1 - D_{\mathrm{d}}$. Since we consider the control of the boost converter around the equilibrium point, we can neglect the

nonlinear term of the converter model and obtain a linearized augmented model as in (4), where the system matrices are as follows:

$$A = \begin{bmatrix} 0 & -\frac{D'_\mathrm{d}}{L} & 0 \\ \frac{D'_\mathrm{d}}{C} & -\frac{1}{RC} & 0 \\ 0 & -1 & 0 \end{bmatrix} \qquad B_u = \begin{bmatrix} \frac{V_\mathrm{g}}{D'_\mathrm{d}L} \\ -\frac{V_\mathrm{g}}{(D'^2_\mathrm{d}R)C} \\ 0 \end{bmatrix}. \qquad (12)$$

We consider that the load R and the duty-cycle D'_d at the operating point are uncertain parameters. Since the boost converter matrices A and B_u do not depend linearly on the uncertain parameters D'_d and R, we define two new uncertain variables $\delta = 1/D'_\mathrm{d}$ and $\beta = 1/(D'^2_\mathrm{d}R)$, in order to meet with a linear dependence. Thus, the parameter vector is defined as $p = [1/R \quad D'_\mathrm{d} \quad \delta \quad \beta]$. The components of the parameter vector are restricted inside the following intervals:

$$\begin{aligned} 1/R &\in [1/R_\mathrm{max}, 1/R_\mathrm{min}] \\ D'_\mathrm{d} &\in [D'_{\mathrm{d\,min}}, D'_{\mathrm{d\,max}}] \\ \delta &\in \left[1/D'_{\mathrm{d\,max}}, 1/D'_{\mathrm{d\,min}}\right] \\ \beta &\in \left[1/\left(D'^2_{\mathrm{d\,max}}R_\mathrm{max}\right), 1/\left(D'^2_{\mathrm{d\,min}}R_\mathrm{min}\right)\right]. \end{aligned} \qquad (13)$$

Note that the uncertain model is inside a polytopic domain formed by $N = 2^4$ vertices.

The introduction of these new parameters δ and β implies a relaxation in the uncertainty constraints, since we assume the independence between uncertain parameters in order to have linear relations. Consequently, the new relaxed model considers dynamic responses that do not correspond to any real case. Therefore, we will obtain a potentially more conservative solution.

In the following sections, we will derive a control law which assures an upper bound of the cost index at the model description vertices, and therefore for all possible cases of the uncertain boost converter.

III. LMI Formulation of the LQR Problem

This section presents the key concepts of the robust LQR control method proposed in this paper. First of all, we introduce the basic result of quadratic stability in form of LMI and its relation with polytopic uncertainty. Second, we will formulate the uncertain LQR problem in form of LMI. These concepts will be applied in Section IV to derive an LQR controller for a buck and a boost converter.

A. Quadratic Stability of an Uncertain Plant

Given a linear time-invariant system

$$\dot{x} = A\,x \qquad (14)$$

it is well known that Lyapunov theory states that the existence of a matrix $\mathbf{P}$ such that the quadratic function

$$V(x) = x'\mathbf{P}x > 0 \qquad \forall\, x \neq 0 \qquad (15)$$

which satisfies

$$\dot{V}(x) = x'(A'\mathbf{P} + \mathbf{P}A)x < 0 \qquad \forall\, x \neq 0 \qquad (16)$$

is a necessary and sufficient condition to assure that the system is quadratically stable (i.e., all trajectories converge to zero) [15]. In the following, we will write $\mathbf{P} > \mathbf{0}$ to note that the matrix $\mathbf{P}$ is positive definite. If there exists a $\mathbf{P} > \mathbf{0}$ such that

$$\dot{V}(x) = x'\left(A'_i\mathbf{P} + \mathbf{P}A_i\right)x < 0 \qquad \forall\, x \neq 0; \qquad \forall\, i = 1, \ldots, N \qquad (17)$$

where A_i are the vertices of a polytopic model $\mathrm{Co}\{\mathcal{G}_1, \ldots, \mathcal{G}_N\}$ defined in the previous section, then it is assured quadratic stability for any plant inside the uncertainty range (see, for example, [25]).

In the inequality (16), $\mathbf{P}$ is the matrix variable (noted in bold notation) that must be found to assure quadratic stability. This inequality is an LMI since it presents linear dependence on the variable and can be solved by convex optimization methods.

We will take advantage of such convex optimization methods that have been implemented in computer algorithms [20], [21], not only to assure quadratic stability of the system but also to solve the LMIs that arise in the LQR control of a switched-mode dc–dc converter.

B. LQR Problem

We are interested in an LMI formulation of the LQR problem, adapted from [27].

Given the system presented in (4), the optimal LQR controller is obtained by using the state-feedback gain $\mathbf{K}$ ($\tilde{u} = \mathbf{K}\tilde{x}$) that minimizes a performance index

$$J = \int_0^\infty (\tilde{x}'Q_\mathrm{w}\tilde{x} + \tilde{u}'R_\mathrm{w}\tilde{u})dt \qquad (18)$$

where Q_w is a symmetric and semidefinite positive matrix and R_w is a symmetric and definite positive matrix. The pair $(A \quad B_u)$ must be controllable.

The LQR problem can be viewed as the weighted minimization of a linear combination of the states $\tilde{x}$ and the control input $\tilde{u}$. The weighting matrix Q_w establishes which states are to be controlled more tightly than others. R_w weights the amount of control action to be applied depending on how large is the deviation of the state $\tilde{x}_i$. This optimization cost weight constraints the magnitude of the control signal.

The LQR controller is obtained by using the feedback gain $\mathbf{K}$ such that, in closed loop, the performance index (18) is rewritten

$$J = \int_0^\infty (\tilde{x}'(Q_\mathrm{w} + \mathbf{K}'R_\mathrm{w}\mathbf{K})\tilde{x})\,dt. \qquad (19)$$

By using the trace operator $\mathbf{Tr}(\cdot)$, which satisfies $a'Xb = \mathbf{Tr}(Xba')$, the performance index is equivalent to

$$\begin{aligned} J &= \int_0^\infty \mathbf{Tr}\left((Q_\mathrm{w} + \mathbf{K}'R_\mathrm{w}\mathbf{K})\tilde{x}\tilde{x}'\right)dt \\ &= \mathbf{Tr}\left((Q_\mathrm{w} + \mathbf{K}'R_\mathrm{w}\mathbf{K})\mathbf{P}\right) \end{aligned} \qquad (20)$$

where $\mathbf{P} = \int_0^\infty (\tilde{x}\tilde{x}')dt$ is a definite positive symmetric matrix that will satisfy

$$(A + B_u\mathbf{K})\mathbf{P} + \mathbf{P}(A + B_u\mathbf{K})' + \tilde{x}_0\tilde{x}_0' = 0 \qquad (21)$$

where $\tilde{x}_0$ represents the state initial condition.

The optimal feedback gain $\mathbf{K}$ can be found by minimization of the following expression:

$$\min_{\mathbf{P},\mathbf{K}} \quad \mathbf{Tr}(Q_w\mathbf{P}) + \mathbf{Tr}\left(R_w^{\frac{1}{2}}\mathbf{K}\mathbf{P}\mathbf{K}'R_w^{\frac{1}{2}}\right)$$

subject to

$$(A + B_u\mathbf{K})\mathbf{P} + \mathbf{P}(A + B_u\mathbf{K})' + \tilde{x}_0\tilde{x}_0' < \mathbf{0}. \qquad (22)$$

Nevertheless, (22) is not linear because the objective function involves the multiplication of variables $\mathbf{P}$ and $\mathbf{K}$. In [27], it is shown that introducing a new variable $\mathbf{Y} = \mathbf{KP}$, we can rewrite (22) as follows:

$$\min_{\mathbf{P},\mathbf{Y}} \quad \mathbf{Tr}(Q_w\mathbf{P}) + \mathbf{Tr}\left(R_w^{\frac{1}{2}}\mathbf{Y}\mathbf{P}^{-1}\mathbf{Y}'R_w^{\frac{1}{2}}\right)$$

subject to

$$A\mathbf{P} + \mathbf{P}A' + B_u\mathbf{Y} + \mathbf{Y}'B_u' + \tilde{x}_0\tilde{x}_0' < \mathbf{0}. \qquad (23)$$

The inequality $(A + B_u\mathbf{K})\mathbf{P} + \mathbf{P}(A + B_u\mathbf{K})' + \tilde{x}_0\tilde{x}_0' < \mathbf{0}$ is homogeneous concerning matrices $\mathbf{P}$ and $\mathbf{Y}$, i.e., for any matrices $\mathbf{P}^*$ and $\mathbf{Y}^*$ satisfying this LMI, $\mu\mathbf{P}^*$ and $\mu\mathbf{Y}^*$, with $\mu > 0$, will also fulfill the inequality. Note that in this case, $\mathbf{K} = \mathbf{YP}^{-1}$ will not depend on the magnitude of μ [28]. Therefore, if the pair $(A\tilde{x}_0)$ is controllable, the LMI can be rewritten as $(A + B_u\mathbf{K})\mathbf{P} + \mathbf{P}(A + B_u\mathbf{K})' + \mathbb{1} < \mathbf{0}$.

In addition, in [27], it is shown that the nonlinear term $\mathbf{Tr}(R_w^{1/2}\mathbf{Y}\mathbf{P}^{-1}\mathbf{Y}'R_w^{1/2})$ can be replaced by a second auxiliary variable $\mathbf{X}$

$$\min_{\mathbf{X}} \quad \mathbf{Tr}(\mathbf{X}) \qquad \text{subject to} \quad \mathbf{X} > R_w^{\frac{1}{2}}\mathbf{Y}\mathbf{P}^{-1}\mathbf{Y}'R_w^{\frac{1}{2}} \quad (24)$$

which, in turn, can be decomposed by Schur's complement (see [15, Ch. 1])

$$\mathbf{X} > R_w^{\frac{1}{2}}\mathbf{Y}\mathbf{P}^{-1}\mathbf{Y}'R_w^{\frac{1}{2}} \quad \leftrightarrow \quad \begin{bmatrix} \mathbf{X} & R_w^{\frac{1}{2}}\mathbf{Y} \\ \mathbf{Y}'R_w^{\frac{1}{2}} & \mathbf{P} \end{bmatrix} > \mathbf{0}. \quad (25)$$

Therefore, the complete LMI formulation of the LQR problem is

$$\min_{\mathbf{P},\mathbf{Y},\mathbf{X}} \quad \mathbf{Tr}(Q_w\mathbf{P}) + \mathbf{Tr}(\mathbf{X})$$

subject to

$$A\mathbf{P} + \mathbf{P}A' + B_u\mathbf{Y} + \mathbf{Y}'B_u' + \mathbb{1} < \mathbf{0}$$

$$\begin{bmatrix} \mathbf{X} & R_w^{\frac{1}{2}}\mathbf{Y} \\ \mathbf{Y}'R_w^{\frac{1}{2}} & \mathbf{P} \end{bmatrix} > \mathbf{0} \qquad \mathbf{P} > \mathbf{0}. \qquad (26)$$

Once this minimization under constraints is solved, the optimal LQR controller can be recovered by $\mathbf{K} = \mathbf{YP}^{-1}$.

Thus, we can formulate the classical LQR problem as a convex optimization problem. The main advantage of this formula-

TABLE I
BUCK CONVERTER PARAMETERS

Parameter	Value
R	[5 , 50] Ω
v_o (V_{ref})	12 V
V_g	[19.2 , 28.8] V
C	200 μF
L	200 μH
T_s	10 μs

tion is that the solution may include uncertainty while classical LQR control is only valid for systems without uncertainty. As shown in the previous section, the extension to consider the polytopic uncertainty model consists on replacing the constraint involving matrices A and B_u with N constraints corresponding to the vertices of the polytope A_i and B_{ui}.

IV. DESIGN EXAMPLES

In this section, we show two examples of robust LQR control solved via LMIs applied to power converters, in order to illustrate the versatility of the presented framework. In the first case, we design the LQR control of a step-down converter, taking into account load and input voltage uncertainty. This example emphasizes the control effort limitations due to the switching nature of power converters. The second example proposes an LQR control for a step-up converter, allowing working condition uncertainty. The boost converter is a nonlinear system whose linearization yields a nonminimum phase model. The main concern in this example will be to assure robust stability with an upper cost bound of the performance index.

A. Robust LQR Control of a PWM Buck Converter

As a first example, we propose to find the robust LQR controller for an uncertain buck converter. In order to preserve simplicity, there are no additional restrictions. The LQR controller is found by optimization of the polytopic version of (26) with the polytopic model defined in (10).

The values of converter parameter set are shown in Table I. The nominal values of the load and the supply voltage are 25 Ω and 24 V, respectively. Stability and an upper cost bound are assured for loads between 5 and 50 Ω and supply voltages in $24 \pm 20\%$ V. The resulting controller is quadratically stable for arbitrarily fast changes of the uncertain parameters [22], which is of interest in presence of switched loads or fast-varying supply sources.

The performance index, and concretely the cost weights Q_w and R_w, are selected such that the control signal enforces the integral action $\tilde{x}_3$ and also the regulated output voltage $\tilde{v}_C$. It is important to remark that measurable states v_C and i_L will contain high-frequency ripple. The inductor ripple at the switching frequency is specially large, and it cannot be completely filtered without modifying the dynamics. In this case, the performance weights are particularly useful, in order to obtain a smooth enough control signal.

In order to exemplify this issue, we have obtained robust LQR controllers for the two following sets of weighting
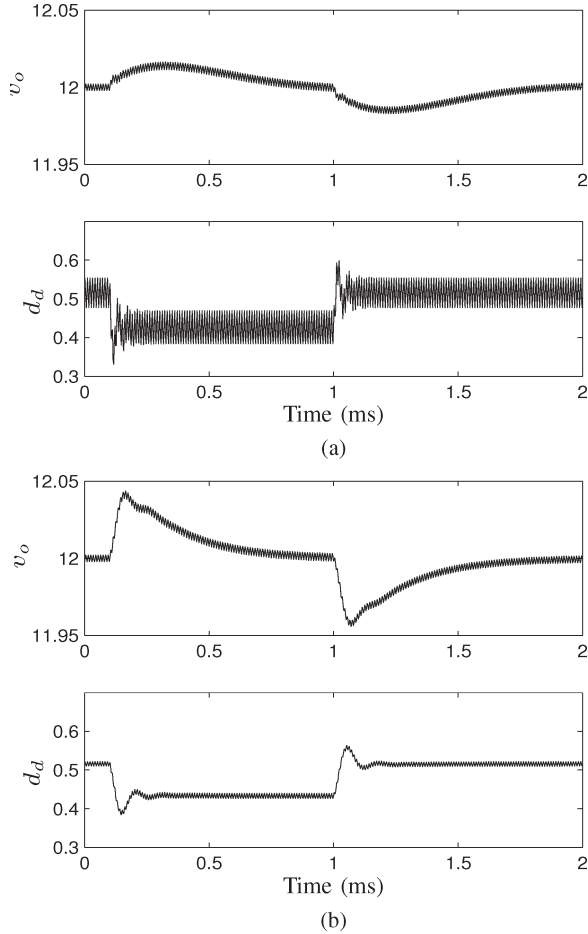
Fig. 4. Simulated transient of the nominal buck converter in presence of a input voltage perturbation of ± 4.8 V, with controllers (a) K_a and (b) K_b.

matrices:

$$Q_{\mathrm{wa}} = \begin{bmatrix} 1 \cdot 10^1 & 0 & 0 \\ 0 & 1 & 0 \\ 0 & 0 & 2 \cdot 10^8 \end{bmatrix} \qquad R_{\mathrm{wa}} = 1$$

$$Q_{\mathrm{wb}} = \begin{bmatrix} 1 \cdot 10^{-1} & 0 & 0 \\ 0 & 10 & 0 \\ 0 & 0 & 2 \cdot 10^8 \end{bmatrix} \qquad R_{\mathrm{wb}} = 2. \quad (27)$$

Using a standard interior points optimization algorithm [20], the state-feedback controllers for the given performance indexes $(Q_{\mathrm{wa}}, R_{\mathrm{wa}})$ and $(Q_{\mathrm{wb}}, R_{\mathrm{wb}})$ are

$$K_a = \begin{bmatrix} -3.25 & -3.96 & 14\,046.05 \end{bmatrix}$$
$$K_b = \begin{bmatrix} -0.48 & -1.86 & 7049.38 \end{bmatrix}. \quad (28)$$

Matrices Q_{wa} and Q_{wb} present different gains for the state variables $\tilde{i}_L$ and $\tilde{v}_C$, while the control effort coefficient is $R_{\mathrm{wb}} = 2R_{\mathrm{wa}}$. As a result, K_b presents smaller gains than K_a. The performance of both controllers is compared in Fig. 4, in which we present the results of a PSIM simulation of the nominal switched converter in presence of an input voltage perturbation of ± 4.8 V. It can be observed in controller K_a that a smaller restriction of the control effort allows a better rejection of perturbations. However, the duty-cycle control signal propagates

Parameter	Value
R	$[10 \, , \, 50] \; \Omega$
D'_d	$[0.3 \, , \, 0.7]$
δ	$[1.42 \, , \, 3.33]$
β	$[0.04 \, , \, 1.11]$
$v_o \; (V_{ref})$	24 V
V_g	12 V
C	200 μF
L	100 μH
T_s	2.5 μs

a larger ripple of the state variables, which may result in an impractical controller for experimental implementation.

Therefore, the choice of a performance index will have influence in the duty-cycle bandwidth. The effect of the ripple propagation has been investigated in [29] and [30], where it was shown that a ripple index d_{dripple}/V_M less than approximately 0.2 (20% of V_M) avoids the nonlinear behaviors of the PWM circuitry. Thanks to LQR control matrices Q_{w} and R_{w}, we can modify the influence of noisy states directly, in contrast with other approaches in which control effort must be limited indirectly.

In the next section, we will describe the LQR controller design for a boost converter, whose linearized model is highly uncertain due to its nonlinear nature.

B. Robust LQR Control of a PWM Boost Converter

As in the previous section, the design of a robust control for a boost converter consists of solving the polytopic version of optimization problem (26) for the parameter set shown in Table II.

Matrices A_i, B_{ui} now correspond to the vertices of the polytopic uncertainty model of the boost converter, which was defined in Section II-B. The nominal values of the converter parameters are $R = 25 \, \Omega$ and $D'_d = 0.5$. The uncertain variables δ and β, defined in (13), belong to the intervals [1.42, 3.33] and [0.04, 1.11], respectively. The main concern of this example is to assure robust stability in a broad range of operation, since the changes in the steady state duty-cycle D'_d cause important variations of the converter dynamics. In order to demonstrate the advantages of the LMI approach, we will compare the robust LQR controller with a conventional LQR without uncertainty.

In this case, note that the boost converter model is bilinear (1) and, in closed loop, can be written as

$$\dot{\tilde{x}}(t) = (A + B_u K + B_n \tilde{x}(t) K) \, \tilde{x}(t) \quad (29)$$

where $B_n = A_{\mathrm{on}} - A_{\mathrm{off}}$, A, B_u are defined in (12) and A_{on}, A_{off} are defined in (11). Consequently, the stability properties of the system with these controllers are local. Once a controller for the linear model has been found, the states inside the region of attraction of the nonlinear system satisfy

$$(A + B_u K + B_n \tilde{x}(t) K) \, P$$
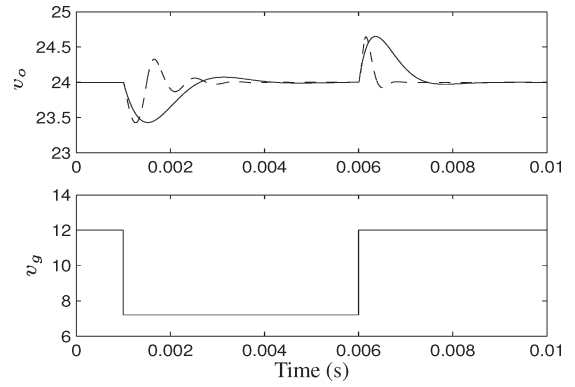$$+ P \, (A + B_u K + B_n \tilde{x}(t) K)' + \mathbb{I} < 0 \quad (30)$$

Fig. 6. Simulated transient of the boost converter in presence of an input voltage perturbation, with (solid line) the robust LQR controller $K_{\mathrm{LMI-LQR}}$ and (dashed line) the nonrobust LQR controller K_{LQR}. Top waveform: output voltage. Bottom waveform: supply voltage.
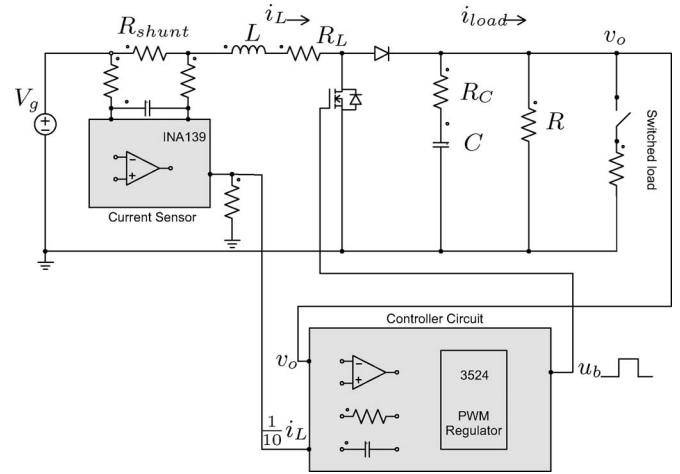

Fig. 7. Implementation diagram of a boost converter with state-feedback regulation.

where $B_n \tilde{x}(t) K$ is the bilinear term that was neglected in the linearization.

Weight matrices of the performance index, Q_{w} and R_{w}, are chosen such that the integral action is enforced and that the control duty-cycle ripple is lower than 5% of the PWM ramp amplitude $V_M = 1$

$$Q_{\mathrm{w}} = \begin{bmatrix} 1 \cdot 10^{-3} & 0 & 0 \\ 0 & 1 \cdot 10^{-3} & 0 \\ 0 & 0 & 1 \cdot 10^{7} \end{bmatrix} \qquad R_{\mathrm{w}} = 1. \qquad (31)$$

The conventional LQR controller for this performance index and the nominal plant is found using the *lqr* MATLAB command. The resulting controller gain vector is

$$K_{\mathrm{LQR}} = [-0.12 \quad -0.53 \quad 3162.28]. \qquad (32)$$

On the other hand, in the uncertain case, we obtain the robust LQR controller by solving (26) with the polytopic uncertainty framework. The resulting controller gain vector is

$$K_{\mathrm{LMI-LQR}} = [-0.86 \quad -1.39 \quad 3159.54]. \qquad (33)$$

Fig. 5. Simulated transient of the boost converter under a load step transient with (solid line) the robust LQR controller $K_{\mathrm{LMI-LQR}}$ and (dashed line) the nonrobust LQR controller K_{LQR}. (a) Load step of 0.48 A under nominal condition $D'_{\mathrm{d}} = 0.5$. (b) Load step of 0.48 A out of nominal condition $D'_{\mathrm{d}} = 0.3$. (c) Load step of 1.44 A under nominal condition $D'_{\mathrm{d}} = 0.5$. (d) Load step of 1.44 A out of nominal condition $D'_{\mathrm{d}} = 0.3$.
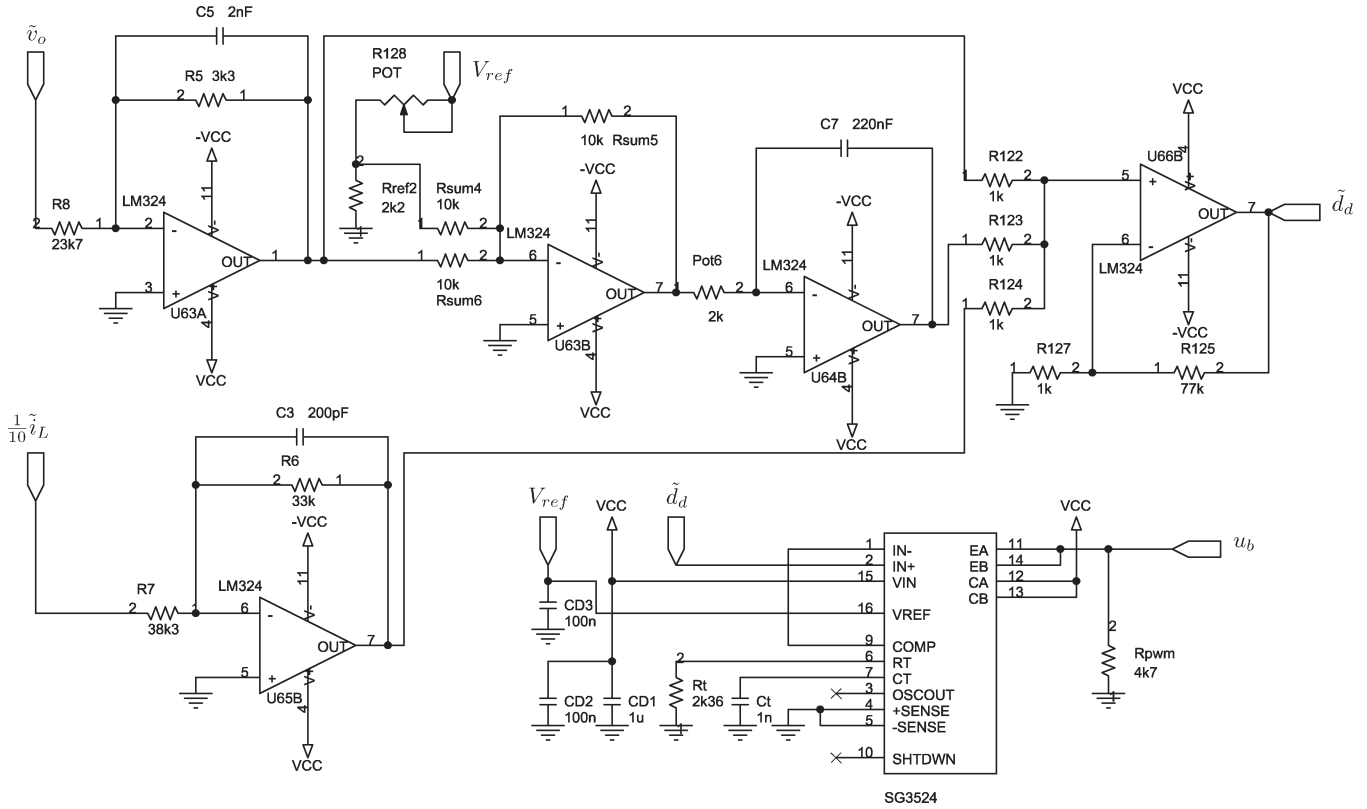
Fig. 8. Detail of the circuit implementation of the robust LQR controller $K_{\mathrm{LMI-LQR}}$ with the PWM regulator.

It is worth to remark that there exist no remarkable differences between the obtained feedback gain vectors K_{LQR} and $K_{\mathrm{LMI-LQR}}$, despite that the LMI optimization guarantees robust regulation of the uncertain converter, while the classic LQR control only considers the performance index over one plant. Next, we will illustrate their properties in presence of output current perturbations, when the converter operates in and out of nominal conditions. We have performed a set of PSIM simulations with the switched-mode circuit, according to Fig. 3. In the first simulation, we have obtained the transient response under a set of load changes, while, in the second simulation, we have depicted the waveforms under a supply voltage step.

The simulations waveforms with changes in the load have been grouped and shown in Fig. 5. The upper waveform of each figure shows the output voltage signal v_{o}, while the lower waveform depicts the current being delivered to the load i_{load}. The response of the LQR controller K_{LQR} corresponds to the dashed line, while the waveform of our proposed robust LQR controller $K_{\mathrm{LMI-LQR}}$ has been drawn with a solid line. The converter works under nominal duty-cycle ($D'_{\mathrm{d}} = 0.5$) in Fig. 5(a) and (c), while it operates with a nonnominal duty-cycle of $D'_{\mathrm{d}} = 0.3$ in Fig. 5(b) and (d). This change in the duty-cycle equals an input voltage variation of -40%, considering that the output voltage remains constant. In Fig. 5(a) and (b), the converter load is initially the nominal value $R = 25\,\Omega$. At $t = 1$ ms, the load changes to $R = 16.6\,\Omega$, and at $t = 6$ ms, it returns to its initial value. On the other hand, in Fig. 5(c) and (d), the converter reacts to larger load perturbation. In this simulation, the initial value of the load is again the nominal value $R = 25\,\Omega$; at $t = 1$ ms, the load changes to $R = 10\,\Omega$,

which is the maximum load allowed in the design; the load returns to $R = 25\,\Omega$ at $t = 6$ ms.

It is shown in Fig. 5 that voltage regulation in nominal conditions is better with the LQR controller (dashed line), despite that the output voltage starts to deteriorate with the large perturbation of Fig. 5(c) which moves the operation point far from its nominal value. On the contrary, the robust LQR controller is slower but maintains its stability properties despite the large perturbation. It can also be observed that output voltage regulation of the LQR controller devolves out of nominal operation $D'_{\mathrm{d}} = 0.3$: In Fig. 5(b), the controller K_{LQR} shows poor damping under small perturbations; furthermore, it becomes unstable in Fig. 5(d), where we apply the large perturbation. The robust controller $K_{\mathrm{LMI-LQR}}$ works, as expected, with the same stability and damping properties when the operation point is far from its nominal value.

In addition, Fig. 6 shows the transient simulation waveforms under a supply voltage change for the converter working with controller K_{LQR} (dashed line) and $K_{\mathrm{LMI-LQR}}$ (solid line). The converter works under nominal conditions and reacts to a supply voltage change of -40% at $t = 1$ ms. At $t = 6$ ms, the supply voltage returns to its initial value. It is important to remark that the proposed controller $K_{\mathrm{LMI-LQR}}$ achieves the same perturbation rejection level than the nonrobust controller K_{LQR}. The damping of the output voltage with controller $K_{\mathrm{LMI-LQR}}$ is similar to that of the nominal case, whereas with controller K_{LQR}, the output voltage damping depends, in a great extend, on the value of the input voltage.

Finally, it is worth to remark that similar results could be obtained if an optimization criteria different from the LQR

weights is used, as for example, an H_∞ optimization with pole placement or controller norm constraints. Obviously, the effectiveness of a particular controller will depend on the criterion that has been chosen to pose the controller synthesis problem.

In the next section, it is described a prototype implementation of the proposed controller, its response under the same conditions of the previous simulations is presented.

V. CONTROL IMPLEMENTATION AND EXPERIMENTAL RESULTS

In order to verify the results derived in the previous sections, we have built a 100-W boost converter. The structure of the converter with the proposed controller is shown in Fig. 7, where the component values are the same that in Table II. We have used a shunt resistance of $R_{\mathrm{shunt}} = 25$ mΩ and an INA139 differential amplifier to measure the inductor current. The load change experiments have been carried out by means of a voltage-controlled switch. Furthermore, we have implemented an experimental version of controllers K_{LQR} and $K_{\mathrm{LMI-LQR}}$. A detail of controller $K_{\mathrm{LMI-LQR}}$ circuit is shown in Fig. 8.

In Fig. 9, we show transient waveforms of the converter with controller K_{LQR} under the load perturbations simulated in the previous section. It can be observed a perfect agreement between the dashed lines in Fig. 5 and the waveforms in Fig. 9. The differences between Figs. 5(d) and 9(d) are due to the fact that in the experimental case, the duty-cycle saturates at 90%, whereas in the simulation case, the duty-cycle reaches 100%.

The correctness of our approach is verified in Fig. 10, which illustrates the performance of the proposed regulator $K_{\mathrm{LMI-LQR}}$ in presence of the previous load perturbations. Again, the experimental results match accurately the solid lines of the simulations plots shown in Fig. 5.

Furthermore, we have verified the response of the controllers K_{LQR} and $K_{\mathrm{LQR-LMI}}$ to a supply voltage change. The experimental result, shown in Fig. 11, accurately verifies the simulations shown in Fig. 6.

VI. CONCLUSION

This paper has proposed a new robust LQR control method based in LMIs for switching dc–dc converters. The proposed models allow one to consider parametric uncertainty whereas LQR formulation permits to assure an upper bound of a performance index. Therefore, the proposed controller exhibits a more predictable response than a classical LQR controller when operating conditions changes. This controller can be derived by means of computer-aided design tools such as MATLAB.

It is shown that the real robust regulator can be easily implemented by standard components such as OAs, capacitors, and resistors. By using an experimental prototype, it is shown that the behavior in presence of step changes of load and line conditions perfectly agrees with the analytical and computer simulations results.

The approach used here can be extended to other more complex converters such as parallel converters, multilevel converters, ac–dc power factor correction circuits, and dc–ac inverters.
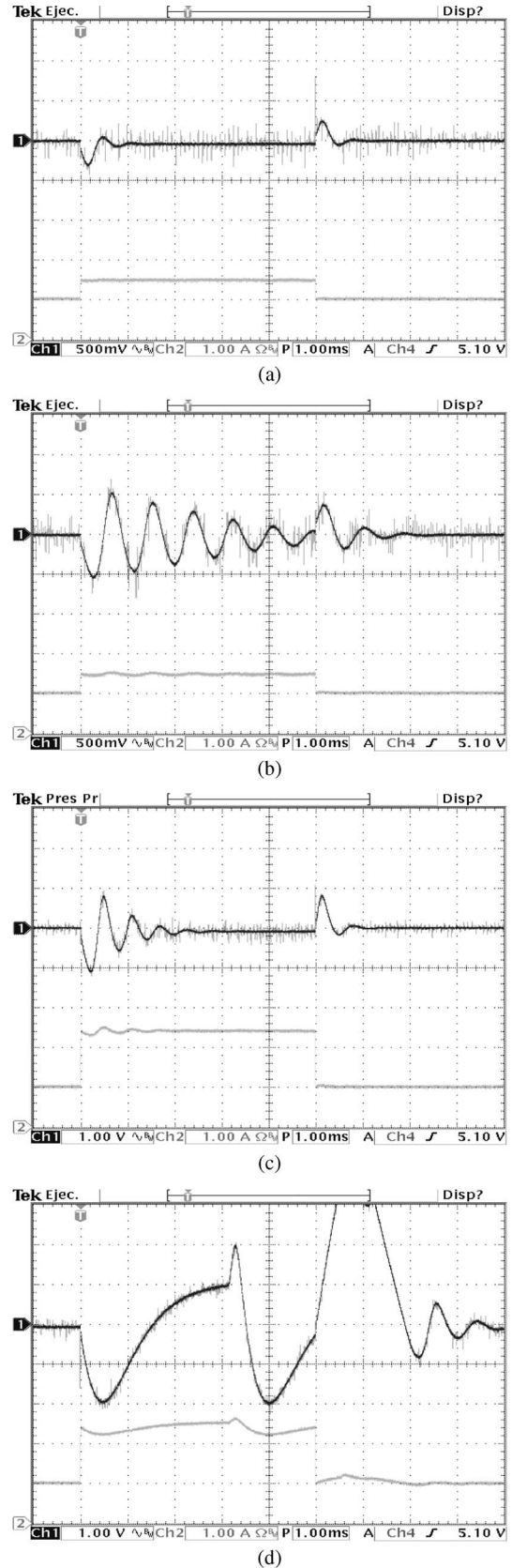

Fig. 9. Experimental transient of the boost converter under a load step transient with the nonrobust LQR controller, K_{LQR}. (a) Load step of 0.48 A under nominal condition $D'_{\mathrm{d}} = 0.5$. (b) Load step of 0.48 A out of nominal condition $D'_{\mathrm{d}} = 0.3$. (c) Load step of 1.44 A under nominal condition $D'_{\mathrm{d}} = 0.5$. (d) Load step of 1.44 A out of nominal condition $D'_{\mathrm{d}} = 0.3$.
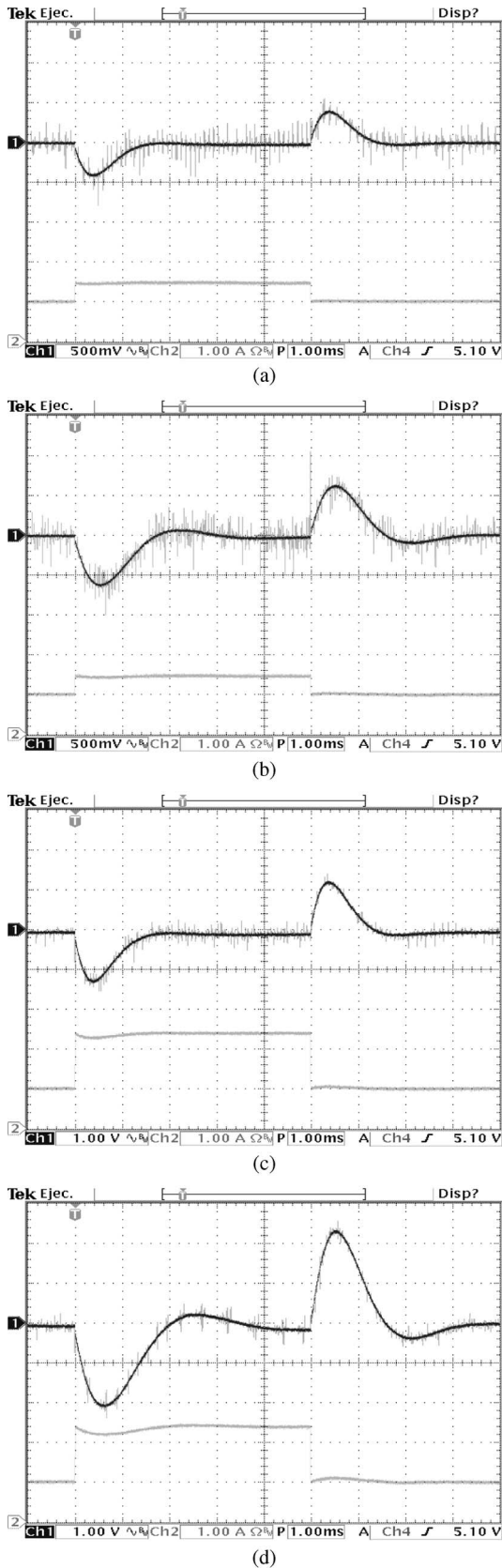
(a)

(b)

(c)

(d)

Fig. 10.   Experimental transient of the boost converter under a load step transient with the robust LQR controller, $K_{\mathrm{LMI-LQR}}$. (a) Load step of 0.48 A under nominal condition $D_{\mathrm{d}}' = 0.5$. (b) Load step of 0.48 A out of nominal condition $D_{\mathrm{d}}' = 0.3$. (c) Load step of 1.44 A under nominal condition $D_{\mathrm{d}}' = 0.5$. (d) Load step of 1.44 A out of nominal condition $D_{\mathrm{d}}' = 0.3$.
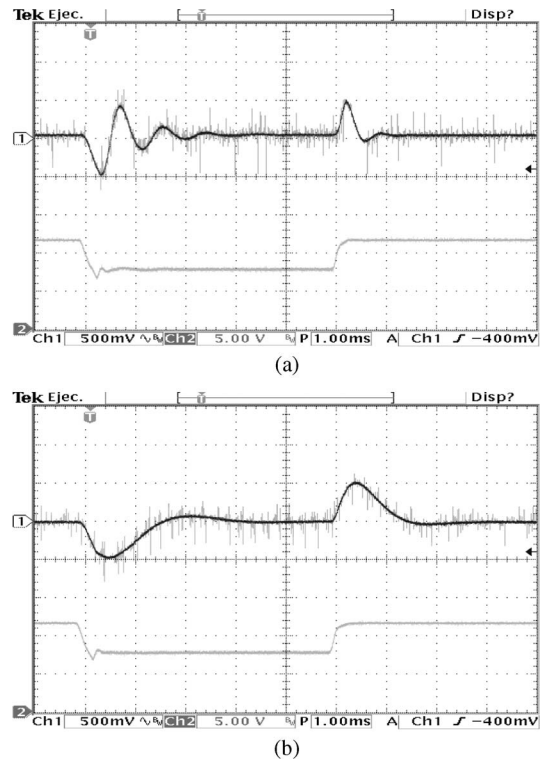

(a)

(b)

Fig. 11.   Experimental transient of the boost converter under a supply voltage step of $\pm 40\%$. (a) With LQR controller K_{LQR}. (b) With robust LQR controller $K_{\mathrm{LMI-LQR}}$.

Future work will deal with the application of the proposed approach to these kinds of systems.

REFERENCES

[1] R. W. Erickson, *Fundamentals of Power Electronics*.   Norwell, MA: Kluwer, 1999.

[2] G. Garcera, A. Abellan, and E. Figueres, "Sensitivity study of the control loops of DC–DC converters by means of robust parametric control theory," *IEEE Trans. Ind. Electron.*, vol. 49, no. 3, pp. 581–586, Jun. 2002.

[3] B. Brad and K. K. Marian, "Voltage-loop power-stage transfer functions with MOSFET delay for boost PWM converter operating in CCM," *IEEE Trans. Ind. Electron.*, vol. 54, no. 1, pp. 347–353, Feb. 2007.

[4] A. G. Perry, G. Feng, Y.-F. Liu, and P. C. Sen, "A design method for PI-like fuzzy logic controllers for DC–DC converter," *IEEE Trans. Ind. Electron.*, vol. 54, no. 5, pp. 2688–2696, Oct. 2007.

[5] M. D. L. del Casale, N. Femia, P. Lamberti, and V. Mainardi, "Selection of optimal closed-loop controllers for DC–DC voltage regulators based on nominal and tolerance design," *IEEE Trans. Ind. Electron.*, vol. 51, no. 4, pp. 840–849, Aug. 2004.

[6] M. H. Todorovic, L. Palma, and P. N. Enjeti, "Design of a wide input range DC–DC converter with a robust power control scheme suitable for fuel cell power conversion," *IEEE Trans. Ind. Electron.*, vol. 55, no. 3, pp. 1247–1255, Mar. 2008.

[7] K. Ogata, *Modern Control Engineering*.   Englewood Cliffs, NJ: Prentice–Hall, 1998.

[8] W. S. Levine, *The Control Handbook*.   Boca Raton, FL: CRC Press, 1996.

[9] *European Cooperation for Space Standardization*, Electrical and Electronic Standard: ECSS-E20A, 2004.

[10] F. H. F. Leung, P. K. S. Tam, and C. K. Li, "The control of switching DC-DC converters—A general LQR problem," *IEEE Trans. Ind. Electron.*, vol. 38, no. 1, pp. 65–71, Feb. 1991.

[11] F. H. F. Leung, P. K. S. Tam, and C. K. Li, "An improved LQR-based controller for switching DC–DC converters," *IEEE Trans. Ind. Electron.*, vol. 40, no. 5, pp. 521–528, Oct. 1993.

[12] C. Gezgin, B. S. Heck, and R. M. Bass, "Control structure optimization of a boost converter: An LQR approach," in *Proc. IEEE PESC*, 1997, vol. 2, pp. 901–907.

[13] R. Boualaga, B. Amar, M. Ammar, and L. A. Loron, "Parameters and states estimation with linear quadratic regulator applied to uninterruptible power supplies (UPS)," in *Proc. IEEE Ind. Electron. Conf.*, 2006, pp. 2055–2060.

[14] C. Jaen, J. Pou, R. Pindado, V. Sala, and J. Zaragoza, "A linear-quadratic regulator with integral action applied to PWM DC–DC converters," in *Proc. IEEE Ind. Electron. Conf.*, 2006, pp. 2280–2285.

[15] S. Boyd, L. El Ghaoui, E. Feron, and V. Balakrishnan, *Linear Matrix Inequalities in Systems and Control Theory*, ser. Studies in Applied and Numerical Mathematics, vol. 15. Philadelphia, PA: SIAM, 1994.

[16] M. Chilali and P. Gahinet, "H_∞ design with pole placement constraints: An LMI approach," *IEEE Trans. Autom. Control*, vol. 41, no. 3, pp. 358–367, Mar. 1996.

[17] S. Tarbouriech, G. Garcia, and A. H. Glattfelder, *Advanced Strategies in Control Systems With Input and Output Constraints*, ser. Lecture Notes in Control and Information Sciences, vol. 346. Berlin, Germany: Springer-Verlag, 2007.

[18] E. A. Johnson and B. Erkus, "Investigation of dissipativity for control of smart dampers via LMI synthesis," in *Proc. ACC*, 2005, vol. 5, pp. 3084–3089.

[19] A. Weinmann, *Uncertain Models and Robust Control*. New York: Springer-Verlag, 1991.

[20] P. Gahinet, A. Nemirovski, A. J. Laub, and M. Chilali, *LMI Control Toolbox for Use With Matlab*. Natick, MA: The MathWorks, Inc., 1995.

[21] J. Sturm, "Using SeDuMi 1.02, a MATLAB toolbox for optimization over symmetric cones," *Optimization Methods and Software*, vol. 11/12, pp. 625–653, 1999. version 1.05. [Online]. Available: http://fewcal.kub.nl/sturm

[22] V. F. Montagner, R. C. L. F. Oliveira, V. J. S. Leite, and P. L. D. Peres, "LMI approach for H_∞ linear parameter-varying state feedback control," *Proc. Inst. Elect. Eng.—Control Theory Appl.*, vol. 152, no. 2, pp. 195–201, Mar. 2005.

[23] *PSIM 6.0*, 2003. [Online]. Available: http://www.powersimtech.com

[24] R. Leyva, A. Cid-Pastor, C. Alonso, I. Queinnec, S. Tarbouriech, and L. Martinez-Salamero, "Passivity-based integral control of a boost converter for large-signal stability," *Proc. Inst. Elect. Eng.—Control Theory Appl.*, vol. 153, no. 2, pp. 139–146, Mar. 2006.

[25] J. Bernussou, P. L. D. Peres, and J. Geromel, "A linear programming oriented procedure for quadratic stabilization of uncertain systems," *Syst. Control Lett.*, vol. 13, no. 1, pp. 65–72, Jul. 1989.

[26] S. Skogestad and I. Postlethwaite, *Multivariable Feedback Control: Analysis and Design*. New York: Wiley, 1996.

[27] E. Feron, V. Balakrishnan, S. Boyd, and L. El Ghaoui, "Numerical methods for H_2 related problems," in *Proc. ACC*, 1992, pp. 2921–2922.

[28] V. B. Larin, "Algorithms of synthesis of controllers by using the procedures both LMI and H_2-optimization," *Appl. Comput. Math.*, vol. 1, no. 2, pp. 190–194, 2002.

[29] A. El Aroudi, E. Alarcon, E. Rodriguez, R. Leyva, G. Villar, F. Guinjoan, and A. Poveda, "Ripple based index for predicting fast-scale instability of dc–dc converters in CCM and DCM," in *Proc. IEEE Ind. Technol. Conf.*, 2006, pp. 1949–1953.

[30] E. Rodriguez, G. Villar, F. Guinjoan, A. Poveda, A. El Aroudi, and E. Alarcon, "General-purpose ripple-based fast-scale instability prediction in switching power regulators," in *Proc. IEEE ISCAS*, 2007, pp. 2423–2426.

Ramon Leyva (M'01) received the Telecommunication Engineering and Ph.D. degrees from the Universitat Politècnica de Catalunya, Barcelona, Spain, in 1992 and 2000, respectively.

He is currently an Associate Professor with the Departament d'Enginyeria en Electrònica, Elèctrica i Automàtica, Universitat Rovira i Virgili, Tarragona, Spain. From March 2002 to March 2003, he held a Visiting Scholarship with the Laboratoire d'Analyse et d'Architecture des Systèmes, Centre National de la Recherche Scientifique, Université de Toulouse, Toulouse, France. His research task is in the field of nonlinear and robust control of power switching converters.

Dr. Leyva serves as Reviewer for several IEEE and Institution of Engineering and Technology scientific publications.

Abdelali El Aroudi (M'00) was born in Tangier, Morocco, in 1973. He received the Graduate degree in physical science from the Faculté des Sciences, Université Abdelmalek Essadi, Tetouan, Morocco, in 1995, and the Ph.D. degree (with honors) from the Universitat Politècnica de Catalunya, Barcelona, Spain, in 2000.

From 1999 to 2001, he was a Visiting Professor in the Department of Electronics, Electrical Engineering and Automatic Control, Technical School of Universitat Rovira i Virgili (URV), Tarragona, Spain, where he became an Associate Professor in 2001 and has been a full-time tenured Associate Professor since 2005. From September 2007 to January 2008, he was a Visiting Scholar with the Department of Mathematics and Statistics, National University of Colombia, Manizales, conducting research on modeling of power electronics circuits for energy management. From February 2008 to July 2008, he was a Visiting Scholar with the Centre de Recherche en Sciences et Technologies de Communications et de l'Informations, Reims, France. He has participated in three Spanish national research projects and five cooperative international projects. His research interests are in the field of structure and control of power conditioning systems for autonomous systems, power factor correction, stability problems, nonlinear phenomena, chaotic dynamics, bifurcations, and control. He has published about 90 papers in scientific journals and conference proceedings. He is a member of the GAEI Research Group, URV, on Industrial Electronics and Automatic Control whose main research fields are power conditioning for vehicles, satellites, and renewable energy.

Dr. El Aroudi is a Reviewer for the IEEE TRANSACTION ON CIRCUITS AND SYSTEMS—I. REGULAR PAPERS, IEEE TRANSACTION ON CIRCUITS AND SYSTEMS—II. EXPRESS BRIEFS, IEEE TRANSACTIONS ON POWER ELECTRONICS, IEEE TRANSACTIONS ON INDUSTRIAL ELECTRONICS, *International Journal of Control*, *International Journal of Power Electronics*, *IET Electric Power Applications*, *International Journal of Systems Science*, *Circuits, Systems and Signal Processing*, *International Journal of Sound and Vibration*, and *Nonlinear Dynamics*. He has given invited talks at several universities in Europe, South America, and Africa.

Carlos Olalla (S'06) received the B.S. degree in automatic control and electronics engineering from the Universitat Rovira i Virgili (URV), Tarragona, Spain, in 2004, and the M.S. degree in advanced automatic control and robotics from the Universitat Politècnica de Catalunya (UPC), Barcelona, Spain, in 2007. He is currently working toward the Ph.D. degree in the Institute of Industrial and Control Engineering (IOC), UPC.

He is also a Research Student with the Grup d'Automàtica i Electrònica Industrial (GAEI) Research Group, Department of Electronics, Electrical Engineering and Automatic Control, URV, where he works on robust control applied to power conditioning for satellites and renewable energy sources. From March 2007 to September 2007, he was a visiting Ph.D. student with the Laboratoire d'Analyse et d'Architecture des Systèmes, Centre National de la Recherche Scientifique, Université de Toulouse, Toulouse, France. His research interests are in uncertainty modeling, robust control synthesis methods, real-time computing, and analog and digital control of power converters.

Isabelle Queinnec received the Ph.D. and HDR degrees in automatic control from the University Paul Sabatier, Toulouse, France, in 1990 and 2000, respectively.

She is currently a Centre National de la Recherche Scientifique (CNRS) Researcher with the Laboratoire d'Analyse et d'Architecture des Systèmes, CNRS, Université de Toulouse, Toulouse. Her current research interests include constrained control and robust control of processes, with particular interest in applications in aeronautical systems, biochemical, and environmental processes.

Dr. Queinnec served as a member of the International Federation of Automatic Control technical committees on "Biosystems and Bioprocesses" in 2002 and "Modelling and Control of Environmental Systems" in 2005.